Title

Pivotal role of MUC1 glycosylation by cigarette smoke in modulating disruption of airway adherens junctions in vitro

Permalink

https://escholarship.org/uc/item/5rn130z4

Journal

The Journal of Pathology, 234(1)

ISSN

0022-3417

Authors

Zhang, Lili
Gallup, Marianne
Zlock, Lorna
et al.

Publication Date

2014-09-01

DOI

10.1002/path.4375

Peer reviewed

Pivotal Role of MUC1 Glycosylation by Cigarette Smoke in Modulating Disruption of Airway Adherens Junctions *In Vitro*

Lili Zhang[1], **Marianne Gallup**[1], **Lorna Zlock**[2], **Yu Ting Feeling Chen**[1], **Walter E. Finkbeiner**[2], and **Nancy A. McNamara**[1,3,4,*]

[1]Francis I. Proctor Foundation, University of California, San Francisco, California

[2]Department of Pathology, University of California, San Francisco, California

[3]Departments of Anatomy and Ophthalmology, University of California, San Francisco, California

[4]School of Optometry and Vision Science Graduate Program, University of California, Berkeley

Abstract

Cigarette smoke increases the risk of lung cancer by 20-fold and accounts for 87% of lung cancer deaths. In the normal airway, heavily O-glycosylated mucin-1 (MUC1) and adherens junctions (AJs) establish a structural barrier that protects the airway from infectious, inflammatory and noxious stimuli. Smoke disrupts cell-cell adhesion via its damaging effects on the AJ protein, epithelial cadherin (E-cad). Loss of E-cad is a major hallmark of epithelial-mesenchymal transition (EMT) and has been reported in lung cancer where it is associated with invasion, metastasis and poor prognosis. Using organotypic cultures of primary human bronchial epithelial (HBE) cells treated with smoke-concentrated medium (Smk), we have demonstrated that E-cad loss is regulated through the aberrant interaction of its AJ binding partner, p120-catenin (p120ctn), and the C-terminus of MUC1 (MUC1-C). Here, we reported that even before MUC1-C became bound to p120ctn, smoke promoted the generation of a novel 400kDa glycoform of MUC1's N-terminus (MUC1-N) differing from the 230kDa and 150kDa glycoforms in untreated control cells. The subsequent smoke-induced, time-dependent shedding of glycosylated MUC1-N exposed MUC1-C as a putative receptor for interactions with EGFR, Src and p120ctn. Smoke-induced MUC1-C glycosylation modulated MUC1-C tyrosine phosphorylation (TyrP) that was essential for MUC1-C/p120ctn interaction through dose-dependent bridging of Src/MUC1-C/galectin-3/ EGFR signalosomes. Chemical deglycosylation of MUC1 using a mixture of N-glycosylation inhibitor tunicamycin and O-glycosylation inhibitor benzyl-α-GalNAc disrupted the Src/MUC1-C/ galectin-3/EGFR complexes and thereby abolished smoke-induced MUC1-C-TyrP and MUC1-C/ p120ctn interaction. Similarly, inhibition of smoke-induced MUC1-N glycosylation using

adenoviral shRNA directed against N-acetyl-galactosaminyl transferase-6 (GALNT6, an enzyme that controls the initiating step of O-glycosylation) successfully suppressed MUC1-C/p120ctn interaction, prevented E-cad degradation and maintained cellular polarity in response to smoke. Thus, GALNT6 shRNA represents a potential therapeutic modality to prevent initiation of events associated with EMT in the smoker's airway.

Keywords

p120-catenin; MUC1; glycosylation; E-cadherin; EGFR; galectin-3; *in vitro* airway model; epithelial-mesenchymal transition; cigarette smoke; lung cancer

Introduction

Lung cancer accounts for 28% of all cancer deaths in the United States and 87% are directly attributable to cigarette smoking [1]. In the U.S. alone, an estimated 45 million current and 45 million former smokers are at high risk for developing lung carcinoma [2]. These numbers ensure that tobacco-related lung cancer will remain a major global health issue for at least the next 50 years and underscore an urgent need to investigate novel diagnostic and therapeutic approaches that can be applied during the earliest stages of lung cancer development.

In the normal airway, apical mucins (MUC) and basolateral adherens junctions (AJs) establish a structural barrier that protects the airway from infectious, inflammatory and noxious stimuli. Epithelial to mesenchymal transition (EMT) causes a morphological change by which cellular polarity and intercellular adhesions are lost and the cell becomes more spindle-shaped, motile and invasive [3,4]. There has been overwhelming evidence demonstrating that EMT is associated with lung cancer. Complete loss, downregulation and mislocalization of AJ proteins E-cadherin (E-cad) and p120-catenin (p120ctn) are observed in all subtypes of lung cancer and are associated with grave prognosis [5,6]. Upon loss of cell polarity in lung cancer, apical MUC1 is repositioned across the entire cell membrane and the levels of depolarized MUC1 predict poor prognosis [7–9]. It is well documented that smoke promotes EMT resulting in loss of cellular polarity, degradation of E-cad, loss of cell-cell adhesion, as well as increased migration of airway epithelial cells [10–15]. Since EMT precedes lung carcinogenesis, identifying and abolishing EMT represents an innovative approach to detect and eradicate lung cancer.

Mucin-1 (MUC1) is a heavily, O-glycosylated transmembrane glycoprotein expressed on the apical surface of mucosal epithelia in the lung, eye, breast and stomach. MUC1 is overexpressed in many epithelial cancers (including lung cancer) where it promotes the immortality and invasion of tumor cells [16]. It is a heterodimeric complex that includes N-terminal (MUC1-N) and C-terminal (MUC1-C) subunits. MUC1-N contains a variable number of tandem repeats (VNTR) and forms the mucin component [17]. The tandem repeats of MUC1-N are serine, threonine and proline (STR) -rich regions, and thereby provide a scaffold to build heavily branched, O-linked glycoproteins. This complex O-glycosylated structure makes up 50–80% of the total mass of MUC1, which can be further complicated by the addition of sulphate and sialic acid residues to create negatively-charged

moieties [18]. Cancer cells express aberrant forms or amounts of O-glycans, which provides ligands that interact with growth factors, lectins, selectins and cell adhesion molecules. The dense layers of O-glycosylation may also help control the local microenvironment and protect cancer cells from adverse growth conditions during invasion and metastasis [18]. Increased O-linked glycosylation of MUC1 including N-acetylgalactosamine (GalNAc, Tn antigen) and sialyl Lewis[X] (SLe[X]) has been reported in lung cancer [19]. Glycosylated MUC1-N shed into the circulation and body cavity are readily detectable in serum and ascites [20]. In fact, serum MUC1-N, referred to as CA15-3, is routinely used in the diagnosis of invasive breast cancer [20] and epithelial ovarian cancer [21].

When glycosylated MUC1-N is released from the cellular surface, it leaves MUC1-C as a putative receptor for interacting with other surface molecules and relaying extracellular stimulation into the interior portion of cells. MUC1-C is composed of extracellular, transmembrane and cytoplasmic tail (MUC1-CT) domains [17]. The extracellular domain of MUC1-C is N-glycosylated at Asn[36] and functions as a binding site for galectin-3, a lectin bridging MUC1-C/EGFR interaction on cellular surface [22]. MUC1-C interacts with numerous kinases, cell adhesion molecules, transcription factors and chaperones that are implicated in malignant transformation [23,24]. During EMT apical MUC1 is repositioned across basolateral membranes, which facilitates MUC1-C's physical interaction with different protein partners [i.e. epidermal growth factor receptor (EGFR)] on the basolateral membrane [16,17].

We have been utilizing an organotypic, 3-dimensional model of human, pseudostratified, polarized, bronchial epithelial cells simulating the *in vivo* airway [25] to study the early events that provoke lung cancer development in response to cigarette smoke. With this approach, we have recapitulated smoke-induced EMT *in vitro* [11–14]. Specifically, we showed that 48 hours of smoke exposure promoted the binding of β-catenin (β-ctn) to MUC1-C, which was chaperoned to the nucleus where it turned on pro-tumor genes via Wnt activation [11]. Yet, even before MUC1-C/β-ctn interaction and activation of pro-tumor signaling, smoke induced the apical repositioning of MUC1-C to basolateral membranes where it interacted with p120ctn to mark the loss of E-cad, liberation of β-ctn from AJs and the initiation of EMT [12]. Here, we show that the aberrant glycosylation and shedding of MUC1-N is an essential event promoting MUC1-C's interaction with p120ctn. Moreover, using inhibitors of MUC1-N glycosylation, we were able to reduce MUC1-C/p120ctn complex formation, preserve AJs and prevent E-cad degradation. These data suggest that aberrant glycosylation of MUC1-N in response to cigarette smoke plays a functional role in the initiation of EMT, thereby serving as an early indicator of malignant transformation, as well as an early therapeutic target in smokers.

Materials and Methods (see supplementary data for details)

Culture and smoke treatment of pseudostratified HBE cells

Pseudostratified HBE cells were established and treated by smoke concentrated medium (Smk) as we described previously [12] and detailed in supplementary data. Tunicamycin [N-acetylglucosamine (GlcNAc) analogue] and benzyl-α-GalNAc (N-acetylgalactosamine analogue) were purchased from Sigma-Aldrich. Target sequence of the synthetic

oligonucleotide for short hairpin RNA (shRNA) against N-acetylgalactosaminotransferase-6 (GALNT6 shRNA) was obtained from a previous report [26] and provided to Applied Biological Materials Inc. (ABM) for synthesizing and subsequent cloning into adenovirus expression vector pSiShuttle. Adenoviral GALNT6 shRNA was further expanded and tittered in ABM. Premade adenoviral shRNA against scrambled control (scrambled shRNA) in pSiShuttle was purchased from ABM.

Human sera and protein analysis

Sera from two non-smokers and two smokers with 35 and 60 pack-year histories were obtained from the Lung Tissue Research Consortium (LTRC; http://www.nhlbi.nih.gov/resources/ltrc.htm). Immunoprecipitation and Western blotting were done as we previously described [12] and detailed in supplementary data. Densitometric quantification of bands was conducted using ImageJ software. MUC1-N shed in Ctrl- and Smk-exposed media was measured with Human CA15-3 ELISA kit (Sigma-Aldrich) following manufacturer's instructions. Immunofluorescence was done as we previously described [12] and detailed in supplementary data. Quantitation of the intensity of GALNT6 IF signals was conducted with Image J software.

Statistical analysis

Three to four independent repeats were conducted in all experiments. Data were presented as mean ± SEM. A Student's t test was used and a p value of < 0.05 was considered statistically significant.

Results

Smoke induces expression and shedding of a 400kDa glycoform of MUC1-N

Pseudostratified HBE cells were incubated with smoke-free (Ctrl) or smoke-conditioned (Smk) medium. Immunoblotting with anti-MUC1-N (VU4H5) specific to the tandem repeat (TR) core domain of MUC1-N revealed three isoforms of 400kDa, 230kDa and 150kDa (Fig. 1A, left panel). In response to smoke, the 150kDa MUC1-N isoform appeared to shift upward toward the 230kDa band beginning at 1h and continuing for 4h of smoke exposure, while the 230kDa isoform shifted upward to form the 400kDa isoform within 2h. The upward shift of MUC1-N was consistent with enhanced glycosylation (Fig. 1C) and resulted in the eventual disappearance of the 150kDa band with only the 230kDa and 400kDa isoforms remaining. A similar shift from 150kDa-to-230kDa and disappearance of the 150kDa isoform was noted in H441 cells after a 2h smoke exposure (Fig. S1A). The 10.7-fold increase in 400kDa MUC1 induced by smoke (Fig. 1A, right panel) was coincident with a 91% reduction in the 150kDa isoform (p < 0.01). The shift from smaller to larger isoform occurred within 2h of smoke exposure and persisted through the 24h exposure (Fig. 1A, left panel). Immunoblotting with anti-MUC1-C (MUC1-CT2) revealed a smear of bands between 20–25kDa that appeared similar before and after Smk treatment (Fig. 1A, left panel).

Smoke provoked a time-dependent accumulation of shed MUC1-N in the culture medium as revealed by human CA15-3 (glycosylated MUC1) ELISA assay (Fig. 1B), thereby

mimicking mucin shedding into the blood and body cavity of human patients that are readily detectable in serum and ascites [20]. We used anti-MUC1-N immunoprecipitation (IP) of Ctrl- or Smk-treated culture medium followed by western blotting (WB) with anti-MUC1-N to confirm that the isoform of MUC1-N shed in response to smoke was the smoke-specific 400kDa band as shown above the ELISA curve in Fig. 1B. The band intensity of shed MUC1-N (Fig. 1B) was lower than the 400kDa MUC1-N in cell lysates (Fig. 1A), suggesting that only a fraction of glycosylated MUC1-N was released into the culture medium upon smoke exposure. Accordingly, in preliminary studies, we used a similar approach to detect the 400kDa isoform of MUC1-N in serum obtained from a long-term smoker that was not apparent in the serum of healthy non-smokers (Fig. 1C). It is important to note that this band was not present in all smokers suggesting its selectivity for a specific population of smokers, rather than simply a biomarker of tobacco smoke exposure.

Since expression of the smoke-specific 400kDa MUC1-N occurred as soon as 2h post-Smk exposure, we hypothesized that smoke-induced O-linked glycosylation in its TR core domain accounted for the rapid switch from the 150kDa to the 400kDa isoform. Cell lysates obtained from Ctrl- and Smk-treated cells were IP'd with anti-MUC1-C followed by WB probed with biotinylated wheat germ agglutinin (WGA; high affinity to N-acetylglucosamine (GlcNAc) and sialic acid moieties), biotinylated vicia villosa lectin (VVA; N-acetylgalactosamine (GalNAc)), anti-MUC1-N and anti-MUC1-C. The 400kDa band recognized by WGA and VVA completely overlapped with the 400kDa isoform of MUC1-N (Fig. 1D, left panel); the 20–25kDa bands recognized by WGA completely overlapped with the 20–25kDa bands of MUC1-C (Fig. 1E, left panel). Densitometric quantitation revealed a 4.7-fold increase of sugar moieties on MUC1-N 400kDa isoform (Fig. 1D, right panel) as well as 2.7-fold increase of sugar moieties on MUC1-C (Fig. 1E, right panel) after 2h. These data confirmed that the smoke-specific, 400kDa MUC1-N isoform is a glycoform of MUC1-N.

Smoke-induced MUC1-C/p120ctn complex formation depends on smoke-provoked MUC1-N and MUC1-C glycosylation

We recently demonstrated the essential role of MUC1-C's interaction with p120ctn in regulating EMT of polarized HBE cells in response to cigarette smoke [12]. Complex formation between MUC1-C and p120ctn occurred after 4h of Smk treatment. Yet, 2h before MUC1-C became bound to p120ctn, we observed aberrant glycosylation of MUC1-N generating the 400kDa glycoform in response to Smk (Fig. 2A). Similar results were noted in H441 cells where increased O-glycosylation of MUC1-N occurred in conjunction with MUC1-C/p120ctn complex formation within 2h of smoke treatment (Fig. S1A). In control HBE cells, AJ protein p120ctn (green) was localized to subapical intercellular junctions displaying the classical pseudostratified epithelial morphology, with MUC1-C (red) localized across the apical surface (Fig. 2B, Ctrl panel). Within 4h of smoke exposure, apical MUC1-C was repositioned to the basolateral membrane and cytoplasm of polarized HBE cells where it interacted with p120ctn (yellow signals indicated by white arrowheads) and provoked loss of p120ctn from AJs (white boxes) (Fig. 2B, Smk panel). MUC1-C/p120ctn complexes were also found in the nuclei where they participated in the regulation of HBE cell proliferation (data not shown). Translocation of MUC1-C occurred in conjunction

with apical-basolateral and cytoplasmic localization of glycosylated MUC1-N (Fig. 2C), which appeared yellow (indicated by yellow arrowheads) when images of MUC1-N (red) and Tn (GalNAc) antigen (green) were overlaid.

To investigate the functional significance of MUC1 glycosylation in response to smoke, polarized HBE cells were preincubated with TB (a mixture of 40ug/ml tunicamycin and 5mM benzyl-α-GalNAc) or vehicle control (DMSO) overnight before exposure to Ctrl or Smk medium for 4h. Benzyl-α-GalNAc inhibits elongation of O-glycans while tunicamycin inhibits N-glycosylation directly and O-glycosylation indirectly when the initial N-glycosylation is a prerequisite of O-glycosylation. In HBE cells treated with TB, the Smk-induced shift of MUC1-N to a 400kDa glycoform was completely abolished (Fig. 2D). Meanwhile the intensity of the 150kDa isoform of MUC1-N was reduced by 50–60% in TB-treated cells versus untreated control (p < 0.05). The 22–25kDa bands of MUC1-C disappeared following TB treatment independent of Smk exposure (Fig. 2D). These data further confirmed that the 400kDa isoform of MUC1-N becomes heavily glycosylated in HBE cells in response to cigarette smoke. Intriguingly, smoke's effect on MUC1-C/p120ctn complex formation was largely abrogated (Fig. 2D) in TB-treated cells. Specifically, smoke provoked a 12-fold increase in MUC1-C bound p120ctn in vehicle control cells while this same interaction in TB-treated cells exposed to smoke was unchanged relative to controls (Fig. 2D). Moreover, tunicamycin treatment alone abolished MUC1-C's glycosylation but failed to affect MUC1-N's glycosylation (Fig. S2), suggesting that MUC1-C is predominantly N-linked. Benzyl-α-GalNAc treatment alone abolished the smoke-specific MUC1-N glycoform while leaving MUC1-C glycosylation intact (Fig. S2). Thus, the smoke-specific glycoform of 400kDa MUC1-N resulted from smoke-provoked O-glycosylation. Interestingly, either tunicamycin or benzyl-α-GalNAc alone abolished MUC1-C/p120ctn interaction (Fig. S2), suggesting that glycosylation of both MUC1-N and MUC1-C are essential to MUC1-C/p120ctn complex formation in response to smoke.

Smoke-induced MUC1-C glycosylation modulates MUC1-C tyrosine phosphorylation (TyrP) through bridging of a MUC1-C/galectin-3/EGFR signalosome complex

We previously showed that smoke-induced tyrosine phosphorylation (TyrP) of MUC1-C was essential to MUC1-C/p120ctn interaction [12]. Since inhibition of MUC1-C glycosylation by TB abrogated smoke-promoted MUC1-C/p120ctn complex formation (Fig. 2D), we investigated whether TB treatment affected MUC1-C-TyrP in response to smoke. Pseudostratified HBE cells were pretreated with TB or vehicle control before exposure to Ctrl or Smk for 4h. Immunoblotting of cell lysates with two different TyrP antibodies revealed a 3.5-fold (PY100) to 2.8-fold (PY20) increase of MUC1-C-TyrP after smoke exposure (Fig. 3A). Immunofluorescent staining confirmed smoke-provoked elevation of MUC1-C-TyrP (yellow signals indicated by yellow arrowheads) by overlaying MUC1-C (red) and PY100/PY20 (green) images (Fig. 3B). MUC1-C-TyrP was localized diffusely along apical, basolateral membranes and intercellular AJs after smoke exposure (Fig. 3B, Smk panel) while it was nearly undetectable in Ctrl cells (Fig. 3B, Ctrl panel). Notably, TB treatment completely abolished smoke-induced MUC1-C-TyrP (Fig. 3A, left panel); densitometric quantitation confirmed that levels of MUC1-C-TyrP in TB- and Smk-treated cells was comparable to untreated control (Fig. 3B, right panel). TB treatment also resulted

in disappearance of MUC1-C 22–25kDa bands (Fig. 3A, left panel), which accounted for a 54% decrease in MUC1-C expression (p < 0.01). Increased MUC1-C degradation secondary to MUC1-C deglycosylation by TB may partially but not completely explain abolished MUC1-C-TyrP in response to smoke.

We have demonstrated that smoke-provoked EGFR/Src/Jnk signaling was upstream of MUC1-C-TyrP [12]. We therefore investigated whether MUC1-C glycosylation was involved in smoke-induced EGFR signaling. We exposed polarized HBE cells with increasing doses of smoke and revealed a dose-dependent increase in complex formation of MUC1-C, EGFR and galectin-3 (Fig. 4A, left panel). Galectin-3 is an intracellular lectin that has been reported to bridge EGFR and MUC1-C interaction [22]. Band quantitation indicated a 2.7-fold increase of EGFR and a 3.1-fold increase of galectin-3 in the MUC1-C complex in response to the maximal dose of Smk versus Ctrl-treated cells (Fig. 4A, right panel). Moreover, the EGFR bound by MUC1-C was a TyrP (activated) form as indicated using the 4G10 anti-TyrP antibody to show a 4.2-fold increase in EGFR-TyrP bound to MUC1-C in response to smoke (Fig. 4A). Similarly, MUC1-C complexes included a TyrP (activated) form of MUC1-C as indicated using three different TyrP antibodies (4G10, PY100 and PY20) with increases in MUC1-C-TyrP ranging from 3.7-fold (PY100) to 4.5-fold (4G10) in response to Smk (Fig. 4A). Immunofluorescent staining of MUC1-C (red)/ galectin-3 (green) (Fig. 4B, left two lanes) and MUC1-C (red)/EGFR (green) (Fig. 4B, right two lanes) confirmed spatial segregation of apical MUC1-C relative to galectin-3/EGFR on basolateral membranes in Ctrl cells, while smoke-promoted the aberrant translocation of MUC1-C, resulting in the colocalization of MUC1-C/galectin-3 and MUC1-C/ EGFR (overlaying yellow signals indicated by yellow arrowheads) along basolateral membranes (Fig. 4B, bottom panels).

Since complex formation between MUC1-C and EGFR appeared to involve bridging via a cytoplasmic sugar, galectin-3 [22], we next investigated whether MUC1-C/EGFR interaction depended on MUC1-C glycosylation. As shown in Fig. 5A, MUC1-C deglycosylation using TB abolished smoke-promoted complex formation of MUC1-C, galectin-3 and EGFR-TyrP in polarized HBE cells. In contrast, the MUC1-C/Src interaction was not affected and thereby occurred independent of MUC1-C glycosylation. Similarly, TB completely abolished smoke-stimulated phosphorylation (activation) of Src (Src-P) and Jnk (Jnk-P), but did not affect smoke-induced EGFR activation (EGFR-TyrP) (Fig. 5B). We have demonstrated previously that smoke-induced EGFR/Src/Jnk signaling was upstream of MUC1-C-TyrP in polarized HBE cells [12]. Here, data indicate that smoke-induced EGFR/Src/Jnk/MUC1-C-TyrP signaling is blocked at EGFR/Src when inhibition of glycosylation using TB disrupts complex formation between MUC1-C/Src and galectin-3/ EGFR.

Suppression of smoke-induced MUC1-N glycosylation abolished smoke-provoked MUC1-C /p120ctn interaction and E-cad loss in polarized HBE cells

We next sought to inhibit smoke-induced MUC1-N glycosylation in an attempt to salvage smoke-promoted AJ damage to the airway epithelium. Enzymes belonging to the N-acetylgalactosamine (GalNAc) transferase (GALNT) family catalyze the initiating step of

mucin-type O-glycosylation in the Golgi apparatus to form GalNAcα1-O-Ser/Thr [27]. Immunofluorescent staining revealed colocalization (overlaying yellow signal indicated by yellow arrowheads) of MUC1-N (red) and GALNT6 (green) in pseudostratified HBE cells independent of smoke exposure: MUC1-N/GALNT6 were predominantly colocalized along the apical surface of Ctrl cells while they were colocalized throughout the basolateral membranes in Smk-exposed cells (Fig. 6A, left two panels). Co-localization (overlaying yellow signals indicated by yellow arrowheads) of Golgi marker 58K (red) and GALNT6 (green) in Ctrl- and Smk-treated cells confirmed that GALNT6 was localized in Golgi complex (Fig. 6A, right two panels) both in the presence and absence of Smk. Since GALNT6 has been reported to O-glycosylate MUC1-N *in vitro* and *in vivo* [26], we hypothesized that MUC1-N was a substrate of GALNT6. To determine whether GALNT6 functionally regulated MUC1-N's O-glycosylation, polarized HBE cells were infected with one multiplicity of infectivity (MOI) of adenoviral GALNT6/scrambled shRNA overnight and cultured for another four days. MUC1-N (red)/GALNT6 (green) co-staining confirmed 80% knocking down of endogenous GALNT6 by GALNT6 shRNA versus scrambled shRNA control (Fig. 6B). Immunoblotting revealed that 1*MOI of GALNT6 shRNA completely abolished the smoke-specific 400kDa MUC1-N that was observed in scrambled shRNA- and Smk-treated cells (Fig. 6C). In addition to abolishing the 400kDa isoform of MUC1-N, 2*MOI of GALNT6 shRNA decreased the 230kDa MUC1-N isoform by 40% (p < 0.05), suggesting the dose-dependent control of GALNT6 in modulating MUC1-N's O-glycosylation (Fig. 6C). GALNT6 silencing failed to reduce MUC1-C's glycosylation in response to smoke (Fig. 6C), confirming that smoke induced N-glycosylation, but not O-glycosylation of MUC1-C, as mentioned above. In line with the data obtained in HBE cells, 1*MOI of GALNT6 shRNA abolished the 230kDa MUC1-N glycoform in H441 cells but did not affect glycosylation of MUC1-C (Fig. S2B).

We next investigated whether suppression of MUC1-N glycosylation using GALNT6 shRNA would reverse EMT initiated by MUC1-C/p120ctn interaction in response to smoke [12]. As expected, abolishing the smoke-specific isoform of 400kDa MUC1-N using 1*MOI of GALNT6 shRNA caused an 82% decrease in MUC1-C/p120ctn complex formation and successfully retained E-cad expression at cell-cell junctions in response to smoke (Fig. 7A). Results were confirmed by immunostaining with MUC1-C (red) and AJ proteins p120ctn, β-ctn and E-cad (all green), indicating that AJ integrity and cellular polarity were maintained in polarized HBE cells exposed to smoke when endogenous GALNT6 expression was compromised by GALNT6 shRNA (Fig. 7B, GALNT6 shRNA + Smk lane versus scrambled shRNA + Smk lane). GALNT6 knockdown also abolished smoke-induced MUC1-C/p120ctn interaction (Fig. S2B and Fig. S2C) and partially preserved junctional p120ctn (Fig. S2C) in H441 cells.

Discussion

We recently demonstrated that smoke promotes EMT through modulating increased complex formation between p120ctn and MUC1-C. MUC1-C/p120ctn interaction in response to smoke occurred in conjunction with the degradation of E-cad and disassembly of AJs, both of which are hallmarks of early lung carcinogenesis [12]. Here, we reported that even before MUC1-C becomes bound to p120ctn, smoke promoted aberrant glycosylation

and shedding of a 400kDa MUC1-N isoform. Blocking MUC1-N's glycosylation led to reduced MUC1-C/p120ctn complex formation and prevented E-cad degradation in response to smoke.

Human MUC1-N contains 20–125 tandem repeats (TR) of 20 amino acids enriched in serine, threonine and proline residues, which gives the molecule the potential for extensive O-glycosylation. The core protein has an estimated molecular weight of 120–225kDa, though the mature glycosylated form ranges from 250–500kDa [28]. WB probed with anti-MUC1-N (VU4H5) specific to the TR core revealed three isoforms of MUC1-N (i.e. 400kDa, 230kDa and 150kDa). The 400kDa MUC1-N isoform was only present in cells exposed to smoke (Fig. 1A). Sugar moieties were demonstrated by WGA staining of the 400kDa band (Fig. 1D). The expression of 400kDa MUC1-N occurred as rapidly as 2h after smoke exposure (Fig. 1A), which was consistent with the median transit time of 142 minutes for MUC1 to be translated, glycosylated and moved to the cell surface in mouse uterine epithelial cells [29]. Moreover, our data demonstrated the subsequent shedding of this isoform from the cell surface, indicated by a time-dependent accumulation of the 400kDa MUC1-N in culture media of HBE cells exposed to smoke (Fig. 1B).

Perhaps most compelling was the presence of the 400kDa glycoform in the serum of a 60 pack-year smoker that was absent in a 35 pack-year smoker, as well as two control patients that had never smoked (Fig. 1C). Although increased levels of MUC1 have been previously detected in the sera of lung cancer patients by CA15-3 ELISA assay [30], we are the first to use WB to show that only the fully glycosylated 400kDa MUC1-N, and not the 150/230kDa isoforms, is present in cell culture media and sera. These data suggested that mature O-glycosylation of the TR domain is either a prerequisite to MUC1-N shedding or confers the shed glycoform of MUC1-N with increased stability. The action of specific sheddases has been reported to mediate shedding of MUC1-N [31,32] and O-glycosylation inhibits degradation of MUC1-N [33]. Since MUC1-N/MUC1-C are non-covalently tethered to the plasma membrane as heterodimers, the release of MUC1-N from HBE cells in response to smoke leaves MUC1-C free to function as a putative receptor for surface molecules [17]. Thus, aberrant O-glycosylation of MUC1-N appears to be among the earliest event of smoke-induced EMT.

Smoke-induced MUC1-C glycosylation mediated EGFR/Src/Jnk/MUC1-C-TyrP signaling through bridging of EGFR/galectin-3/MUC1-C signalosomes. We have shown that in order to interact with p120ctn, MUC1-C must be first activated through TyrP downstream of smoke-promoted EGFR/Src/Jnk signaling [12]. Here, we revealed that apical-basolateral translocation of MUC1-C-TyrP (Fig. 3B) occurred in conjunction with apical-basolateral translocation of MUC1-N-Tn (Fig. 2C), as well as the formation of MUC1-C/p120ctn and EGFR/galectin-3/MUC1-C complexes on basolateral membranes of pseudostratified HBE cells (Fig. 2B and 4B). TB deglycosylation of MUC1-C abrogated MUC1-C/EGFR/galectin-3 complexes but not MUC1-C/Src complexes (Fig. 5A), indicating that the association of MUC1-C to EGFR and galectin-3 depends on glycan crosslinking, while MUC1-C/Src association is more likely due to protein-protein interaction. The extracellular domain of MUC1-C contains three putative N-glycosylation sites at asparagine residues (positions 16, 25 and 36) [22]. Consistent with this, the carbohydrate recognition domain

(CRD) of galectin-3 has been reported to physically bridge N-glycans at Asn[36] of MUC1-C and EGFR [22]. In stage-II non-small cell lung cancer (NSCLC) the level of galectin-3 was an indicator of poor clinical prognosis [34]. The YEKV motif in the cytoplasmic domain of MUC1-C has been reported to be the binding site of Src [35]. Furthermore, TB deglycosylation of MUC1-C did not affect smoke-induced EGFR-TyrP but abolished the Src-P/Jnk-P/MUC1-C-TyrP signaling downstream of EGFR (Fig. 3A and 5B). Thus, galectin-3-mediated MUC1-C/EGFR interaction in response to smoke appears to bring EGFR and Src-bound MUC1-C into proximity to facilitate EGFR-modulated downstream signaling. MUC1 has also been reported to facilitate smoke carcinogen benzo(a)pyrene-induced EGFR signaling through increasing EGFR's half-life from 32min to 145min in HBE cells [36]. Thus, smoke-induced bridging of MUC1-C/galectin-3/EGFR may enhance EGFR signaling by increasing the stability of EGFR. Previous studies provide evidence of an alternative mechanism whereby nuclear MUC1-C may elicit EMT through modulating the activity of different zinc-finger transcription factors in breast (ZEB1) [37], pancreatic (Snail, Slug) [38] and renal (Snail) carcinomas [39]. MUC1-C in complex with androgen receptor has been reported to drive androgen-independent growth and EMT in prostate cancer [40].

The defining features of this signaling pathway and the timing by which it occurred formed the basis of a novel approach to prevent MUC1-C/p120ctn complex formation and Ecad degradation in response to cigarette smoke. Specifically, we used both GALNT6 shRNA delivered via adenovirus (Fig. 6C) and chemical inhibitors of glycosylation (Fig. 2D) to inhibit smoke-induced MUC1-N glycosylation. In the absence of MUC1-N glycosylation, MUC1-C/p120ctn complex formation was prevented (Fig. 2D and 7A). Deglycosylation of MUC1-N by GALNT6 shRNA completely abolished smoke-induced E-cad degradation (Fig. 7A), apical-basolateral translocation of MUC1-C and recovered the spatial segregation of apical MUC1-C and basolateral p120ctn (Fig. 7B). Our data are in consistent with two recent reports: knockdown of GALNT6 resulted in increased E-cad expression and cell adhesion in breast cancer cells [26], while overexpression of GALNT6 disrupted acinar morphogenesis and caused EMT-like cellular changes in normal mammary epithelial cells [41]. These data established the feasibility of GALNT6 shRNA in preventing the initiation of EMT and lung carcinogenesis through blocking MUC1-N's O-glycosylation and subsequent MUC1-C/p120ctn interaction. Taken together, our data suggest that inhibition of MUC1-N glycosylation in smokers represents an early therapeutic target to prevent EMT in lung cancer development.

Supplementary Material

Refer to Web version on PubMed Central for supplementary material.

Acknowledgments

References

1. Society AC. Cancer Facts & Figures 2009. 2009. Internet http://wwwcancerorg/acs/groups/content/
@nho/documents/document/500809webpdfpdf

2. Gilpin EA, Pierce JP. Demographic differences in patterns in the incidence of smoking cessation: United States 1950–1990. Ann Epidemiol. 2002; 12:141–150. [PubMed: 11897171]

3. Polyak K, Weinberg RA. Transitions between epithelial and mesenchymal states: acquisition of malignant and stem cell traits. Nat Rev Cancer. 2009; 9:265–273. [PubMed: 19262571]

4. Mani SA, Guo W, Liao MJ, et al. The epithelial-mesenchymal transition generates cells with properties of stem cells. Cell. 2008; 133:704–715. [PubMed: 18485877]

5. Thoreson MA, Reynolds AB. Altered expression of the catenin p120 in human cancer: implications for tumor progression. Differentiation. 2002; 70:583–589. [PubMed: 12492499]

6. Liu Y, Wang Y, Zhang Y, et al. Abnormal expression of p120-catenin, E-cadherin, and small GTPases is significantly associated with malignant phenotype of human lung cancer. Lung Cancer. 2009; 63:375–382. [PubMed: 19162367]

7. Guddo F, Giatromanolaki A, Koukourakis MI, et al. MUC1 (episialin) expression in non-small cell lung cancer is independent of EGFR and c-erbB-2 expression and correlates with poor survival in node positive patients. J Clin Pathol. 1998; 51:667–671. [PubMed: 9930070]

8. Awaya H, Takeshima Y, Yamasaki M, et al. Expression of MUC1, MUC2, MUC5AC, and MUC6 in atypical adenomatous hyperplasia, bronchioloalveolar carcinoma, adenocarcinoma with mixed subtypes, and mucinous bronchioloalveolar carcinoma of the lung. Am J Clin Pathol. 2004; 121:644–653. [PubMed: 15151204]

9. Situ D, Wang J, Ma Y, et al. Expression and prognostic relevance of MUC1 in stage IB non-small cell lung cancer. Med Oncol. 2011; 28(Suppl 1):S596–604. [PubMed: 21116877]

10. Dasari V, Gallup M, Lemjabbar H, et al. Epithelial-mesenchymal transition in lung cancer: is tobacco the "smoking gun"? Am J Respir Cell Mol Biol. 2006; 35:3–9. [PubMed: 16484682]

11. Chen YT, Gallup M, Nikulina K, et al. Cigarette smoke induces epidermal growth factor receptor-dependent redistribution of apical MUC1 and junctional beta-catenin in polarized human airway epithelial cells. Am J Pathol. 2010; 177:1255–1264. [PubMed: 20651243]

12. Zhang L, Gallup M, Zlock L, et al. Cigarette smoke disrupts the integrity of airway adherens junctions through the aberrant interaction of p120-catenin with the cytoplasmic tail of MUC1. J Pathol. 2013; 229:74–86. [PubMed: 22833523]

13. Zhang L, Gallup M, Zlock L, et al. p120-catenin modulates airway epithelial cell migration induced by cigarette smoke. Biochem Biophys Res Commun. 2012; 417:49–55. [PubMed: 22120634]

14. Zhang L, Gallup M, Zlock L, et al. Rac1 and Cdc42 Differentially Modulate Cigarette Smoke-Induced Airway Cell Migration through p120-Catenin-Dependent and -Independent Pathways. Am J Pathol. 2013; 182:1986–1995. [PubMed: 23562274]

15. Shaykhiev R, Otaki F, Bonsu P, et al. Cigarette smoking reprograms apical junctional complex molecular architecture in the human airway epithelium in vivo. Cell Mol Life Sci. 2011; 68:877–892. [PubMed: 20820852]

16. Kufe DW. Mucins in cancer: function, prognosis and therapy. Nat Rev Cancer. 2009; 9:874–885. [PubMed: 19935676]

17. Kufe DW. Functional targeting of the MUC1 oncogene in human cancers. Cancer Biol Ther. 2009; 8:1197–1203. [PubMed: 19556858]

18. Hollingsworth MA, Swanson BJ. Mucins in cancer: protection and control of the cell surface. Nat Rev Cancer. 2004; 4:45–60. [PubMed: 14681689]

19. Pinto R, Carvalho AS, Conze T, et al. Identification of new cancer biomarkers based on aberrant mucin glycoforms by in situ proximity ligation. J Cell Mol Med. 2012; 16:1474–1484. [PubMed: 21883895]

20. Metzgar RS, Rodriguez N, Finn OJ, et al. Detection of a pancreatic cancer-associated antigen (DU-PAN-2 antigen) in serum and ascites of patients with adenocarcinoma. Proc Natl Acad Sci U S A. 1984; 81:5242–5246. [PubMed: 6591188]

21. Scambia G, Benedetti Panici P, Baiocchi G, et al. CA 15-3 as a tumor marker in gynecological malignancies. Gynecol Oncol. 1988; 30:265–273. [PubMed: 3163666]

22. Ramasamy S, Duraisamy S, Barbashov S, et al. The MUC1 and galectin-3 oncoproteins function in a microRNA-dependent regulatory loop. Mol Cell. 2007; 27:992–1004. [PubMed: 17889671]

23. Singh PK, Hollingsworth MA. Cell surface-associated mucins in signal transduction. Trends Cell Biol. 2006; 16:467–476. [PubMed: 16904320]

24. Senapati S, Das S, Batra SK. Mucin-interacting proteins: from function to therapeutics. Trends Biochem Sci. 2010; 35:236–245. [PubMed: 19913432]

25. Pezzulo AA, Starner TD, Scheetz TE, et al. The air-liquid interface and use of primary cell cultures are important to recapitulate the transcriptional profile of in vivo airway epithelia. Am J Physiol Lung Cell Mol Physiol. 2011; 300:L25–31. [PubMed: 20971803]

26. Park JH, Nishidate T, Kijima K, et al. Critical roles of mucin 1 glycosylation by transactivated polypeptide N-acetylgalactosaminyltransferase 6 in mammary carcinogenesis. Cancer Res. 2010; 70:2759–2769. [PubMed: 20215525]

27. Bennett EP, Mandel U, Clausen H, et al. Control of mucin-type O-glycosylation: a classification of the polypeptide GalNAc-transferase gene family. Glycobiology. 2012; 22:736–756. [PubMed: 22183981]

28. Gendler SJ, Spicer AP. Epithelial mucin genes. Annu Rev Physiol. 1995; 57:607–634. [PubMed: 7778880]

29. Pimental RA, Julian J, Gendler SJ, et al. Synthesis and intracellular trafficking of Muc-1 and mucins by polarized mouse uterine epithelial cells. J Biol Chem. 1996; 271:28128–28137. [PubMed: 8910427]

30. Nutini S, Cappelli G, Benucci A, et al. Serum NSE, CEA, CT, CA 15-3 levels in human lung cancer. Int J Biol Markers. 1990; 5:198–202. [PubMed: 1965544]

31. Lillehoj EP, Han F, Kim KC. Mutagenesis of a Gly-Ser cleavage site in MUC1 inhibits ectodomain shedding. Biochem Biophys Res Commun. 2003; 307:743–749. [PubMed: 12893286]

32. Thathiah A, Blobel CP, Carson DD. Tumor necrosis factor-alpha converting enzyme/ADAM 17 mediates MUC1 shedding. J Biol Chem. 2003; 278:3386–3394. [PubMed: 12441351]

33. Altschuler Y, Kinlough CL, Poland PA, et al. Clathrin-mediated endocytosis of MUC1 is modulated by its glycosylation state. Mol Biol Cell. 2000; 11:819–831. [PubMed: 10712502]

34. Szoke T, Kayser K, Trojan I, et al. The role of microvascularization and growth/adhesion-regulatory lectins in the prognosis of non-small cell lung cancer in stage II. Eur J Cardiothorac Surg. 2007; 31:783–787. [PubMed: 17369045]

35. Li Y, Kuwahara H, Ren J, et al. The c-Src tyrosine kinase regulates signaling of the human DF3/MUC1 carcinoma-associated antigen with GSK3 beta and beta-catenin. J Biol Chem. 2001; 276:6061–6064. [PubMed: 11152665]

36. Xu X, Bai L, Chen W, et al. MUC1 contributes to BPDE-induced human bronchial epithelial cell transformation through facilitating EGFR activation. PLoS One. 2012; 7:e33846. [PubMed: 22457794]

37. Rajabi H, Alam M, Takahashi H, et al. MUC1-C oncoprotein activates the ZEB1/miR-200c regulatory loop and epithelial-mesenchymal transition. Oncogene. 2014; 33:1680–1689. [PubMed: 23584475]

38. Roy LD, Sahraei M, Subramani DB, et al. MUC1 enhances invasiveness of pancreatic cancer cells by inducing epithelial to mesenchymal transition. Oncogene. 2011; 30:1449–1459. [PubMed: 21102519]

39. Gnemmi V, Bouillez A, Gaudelot K, et al. MUC1 drives epithelial-mesenchymal transition in renal carcinoma through Wnt/beta-catenin pathway and interaction with SNAIL promoter. Cancer Lett. 2014; 346:225–236. [PubMed: 24384091]

40. Rajabi H, Ahmad R, Jin C, et al. MUC1-C oncoprotein confers androgen-independent growth of human prostate cancer cells. Prostate. 2012; 72:1659–1668. [PubMed: 22473899]

41. Park JH, Katagiri T, Chung S, et al. Polypeptide N-acetylgalactosaminyltransferase 6 disrupts mammary acinar morphogenesis through O-glycosylation of fibronectin. Neoplasia. 2011; 13:320–326. [PubMed: 21472136]
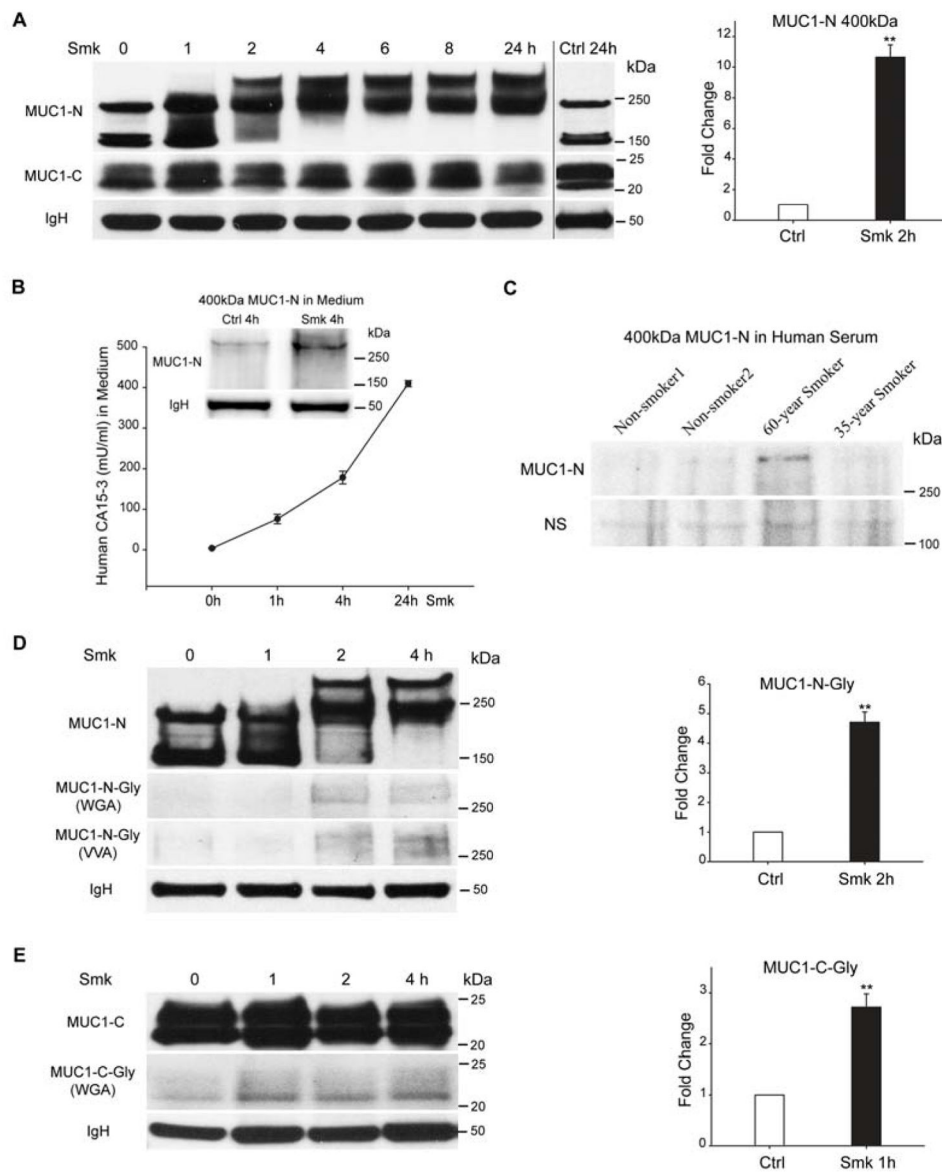
Figure 1.
Smoke induces expression and shedding of a 400kDa glycoform of MUC1-N. **(A)**
Pseudostratified HBE cells exposed to smoke-concentrated medium (Smk) were harvested at
the indicated time points and immunoprecipitated (IP) using an antibody directed against
MUC1-C (MUC1-CT2). MUC1-C IP was probed with antibodies directed against the
tandem repeat core of MUC1-N (VU4H5) and MUC1-C. VU4H5 recognized 400kDa,
230kDa and 150kDa isoforms of MUC1-N, while anti-MUC1-C recognized a smear of
bands between 20kDa and 25kDa. Immunoglobulin heavy chain (IgH) served as the loading
control. Densitometric quantitation of the MUC1-N 400kDa band after a 2h Smk exposure
was normalized to unexposed 0h control (designated as 1-fold) and reported as mean ± SEM
fold changes (**p < 0.01). **(B)** Time-dependent shedding of the smoke-specific 400kDa
MUC1-N isoform. Culture media of polarized HBE cells were collected at indicated times
after Smk exposure. MUC1-N in Smk-exposed media was measured using a human CA15-3

ELISA kit. Results are presented as mU/ml using human CA15-3 standard provided in the kit. Shed MUC1-N was confirmed as the smoke-induced 400kDa band with VU4H5 IP followed by VU4H5 western blotting (WB) as shown in the left corner of the ELISA curve. IgH bands serve as the loading control. **(C)** The 400kDa isoform of MUC1-N was detected in smoker's serum. VU4H5 IP followed by VU4H5 WB was used to look for the presence of MUC1-N in sera obtained from two smokers; one with a smoking history of 60 pack-years and the other with a history of 35 pack-years. Results were compared to two patients who never smoked. The 400kDa isoform of MUC1-N was noted in the serum of the patient with a smoking history of 60 pack-years. Non-specific bands (NS) serve as the loading control. **(D–E)** HBE cells exposed to Smk were harvested at indicated time points, IP'd with anti-MUC1-C and probed with VU4H5, anti-MUC1-C, biotinylated wheat germ agglutinin (WGA; N-acetylglucosamine (GlcNAc) and sialic acid moieties) and biotinylated vicia villosa lectin (VVA; N-acetylgalactosamine (GalNAc)) on MUC1-N and MUC1-C. Equal loading was confirmed by IgH bands. Densitometric quantitation of the glycosylated 400kDa MUC1-N **(D)** and glycosylated MUC1-C **(E)** detected by WGA after a 2h or 1h Smk exposure was normalized to unexposed 0h control (designated as 1-fold) (mean ± SEM fold change; **p < 0.01).
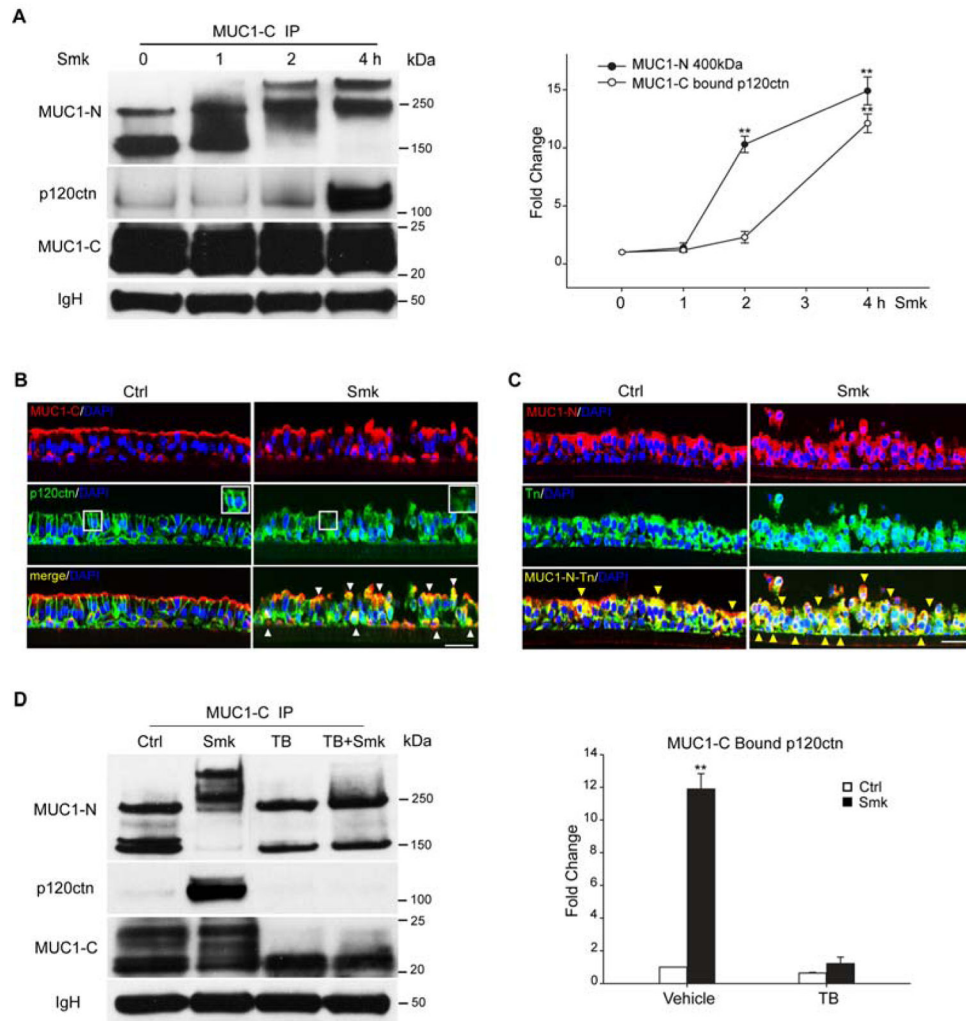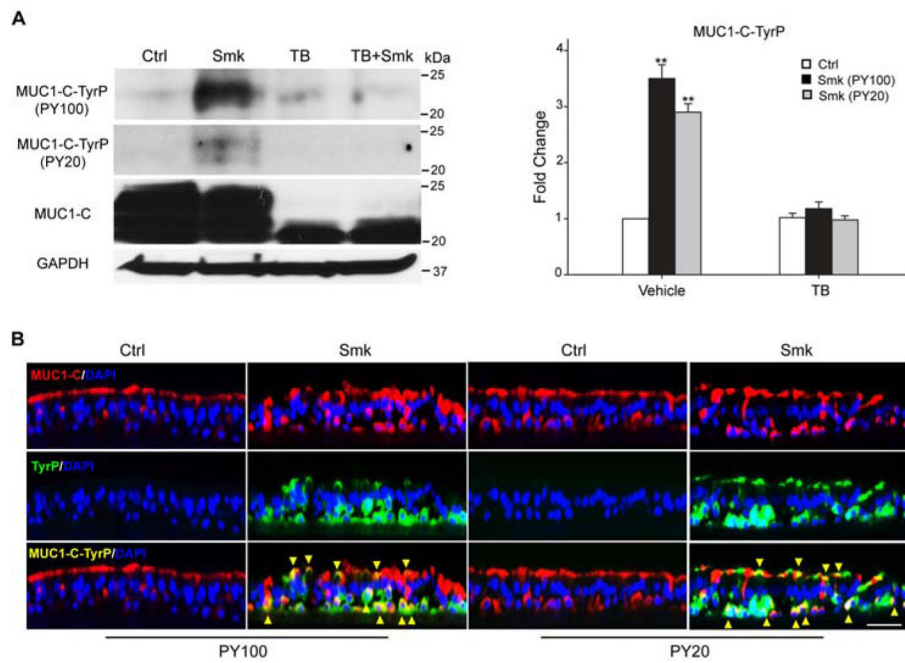
Figure 2.
Smoke-induced MUC1-C/p120ctn interaction depends on MUC1 glycosylation in polarized HBE cells. **(A)** HBE cells exposed to smoke (Smk) were harvested at indicated time points, IP'd using anti-MUC1-C and probed with VU4H5, anti-p120ctn and anti-MUC1-C. IgH bands served as the loading control. Densitometric quantitation of 400kDa MUC1-N and MUC1-C bound p120ctn in Smk-treated cells was normalized to untreated Ctrl (designated 0h as 1-fold) and reported as mean ± SEM fold changes. **p < 0.01, Smk-treated cells versus Ctrl. **(B–C)** HBE cells were stained by immunofluorescence after exposure to Smk and smoke-free medium (Ctrl) for 4h. **(B)** Immunostaining with anti-MUC1-C (red, top panels) and anti-p120ctn (green, middle panels) is shown. White boxes in middle panels indicate p120ctn at intercellular areas, which remains intact in Ctrl cells but predominantly lost in Smk-exposed cells. Merged MUC1-C and p120ctn images (generating yellow signals, bottom panels) demonstrate colocalization of MUC1-C and p120ctn in the cytoplasm and basolateral membranes (white arrowheads) after smoke exposure. **(C)** Staining with anti-MUC1-N (red, top panels) and anti-Tn (anti-GalNAc, green, middle panels). Glycosylated MUC1-N (MUC1-N-Tn, bottom panels) is indicated by overlaying of MUC1-N and Tn

images generating yellow signals (yellow arrowheads). Cell nuclei were visualized with DAPI (blue). Scale bar represents 50μm. **(D)** HBE cells were preincubated with TB [20ug/ml tunicamycin (N-glycosylation inhibitor) and 2mM benzyl-α-GalNAc (O-glycosylation inhibitor)] or vehicle control (DMSO) overnight and exposed to Smk and Ctrl medium for 4h in the presence of TB. MUC1-C IP was analyzed with MUC1-N, MUC1-C and p120ctn antibodies. After TB treatment, anti-MUC1-N recognized the 150kDa and 230kDa isoforms of MUC1-N, while anti-MUC1-C recognized MUC1-C bands between 20kDa and 22kDa. Equal loading was confirmed with IgH. Densitometric quantitation of p120ctn IP'd by MUC1-C in Smk and/or TB-treated cells was normalized to untreated Ctrl (designated as 1-fold) and reported as mean ± SEM fold change. $**p < 0.01$, Smk and/or TB-treated cells versus untreated Ctrl.

Figure 3.
Smoke-induced MUC1-C glycosylation modulates MUC1-C tyrosine phosphorylation (TyrP) in polarized HBE cells. **(A–B)** HBE cells were preincubated with TB or vehicle control (DMSO) overnight before treating with Smk or Ctrl medium for 4h in the presence of TB. **(A)** Cell lysates were analyzed by WB probed with TyrP (PY100 or PY20) antibodies. Blots were stripped and reprobed with MUC1-C antibody. Bands recognized by PY100 and PY20 overlapped with each other and with MUC1-C. Equal loading was confirmed with GAPDH. Densitometric quantitation of MUC1-C-TyrP (PY100) and MUC1-C-TyrP (PY20) after Smk and/or TB treatment was normalized to untreated Ctrl (designed as 1-fold) and reported as mean ± SEM. **p < 0.01, Smk and/or TB-treated cells versus untreated Ctrl. **(B)** Immunostaining with anti-MUC1-C (red, top panels), anti-PY100 (green, middle panels of left two lanes) or anti-PY20 (green, middle panels of right two lanes). Merged MUC1-C and PY100/PY20 images (generating yellow signals, bottom panels) demonstrate smoke-provoked MUC1-C-TyrP (yellow arrowheads). Cell nuclei were visualized with DAPI (blue). Scale bar represents 50μm.
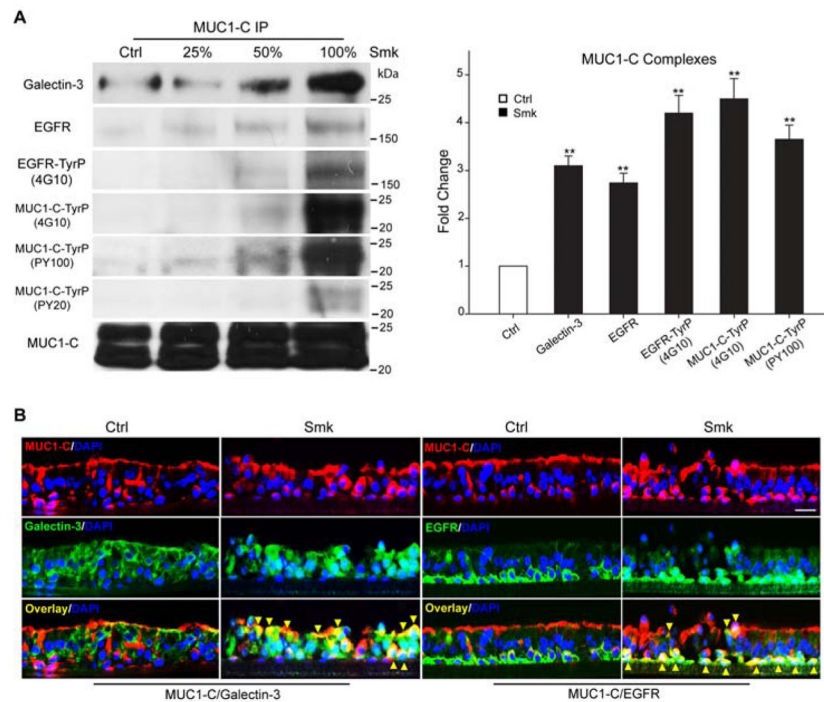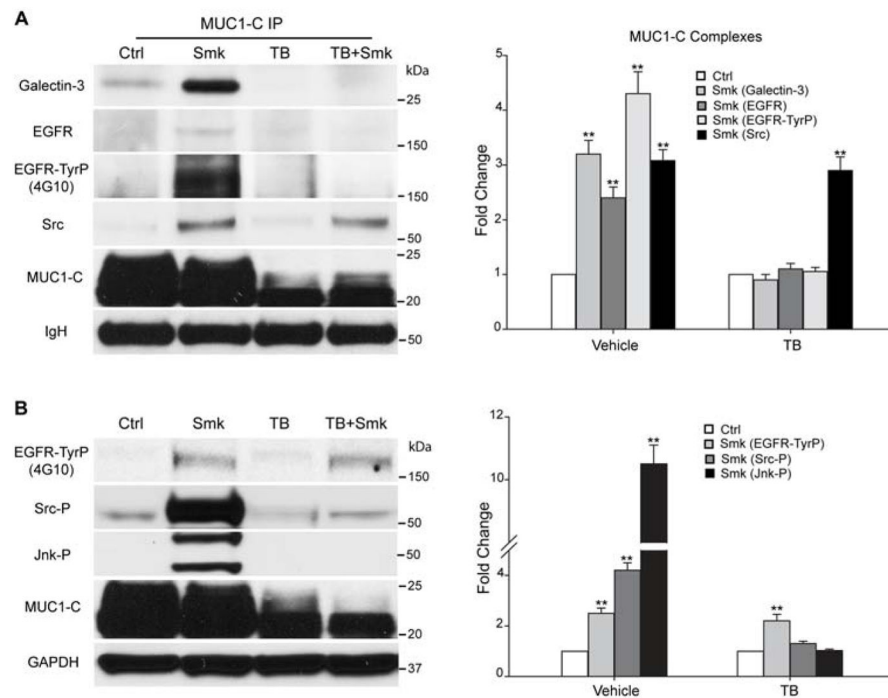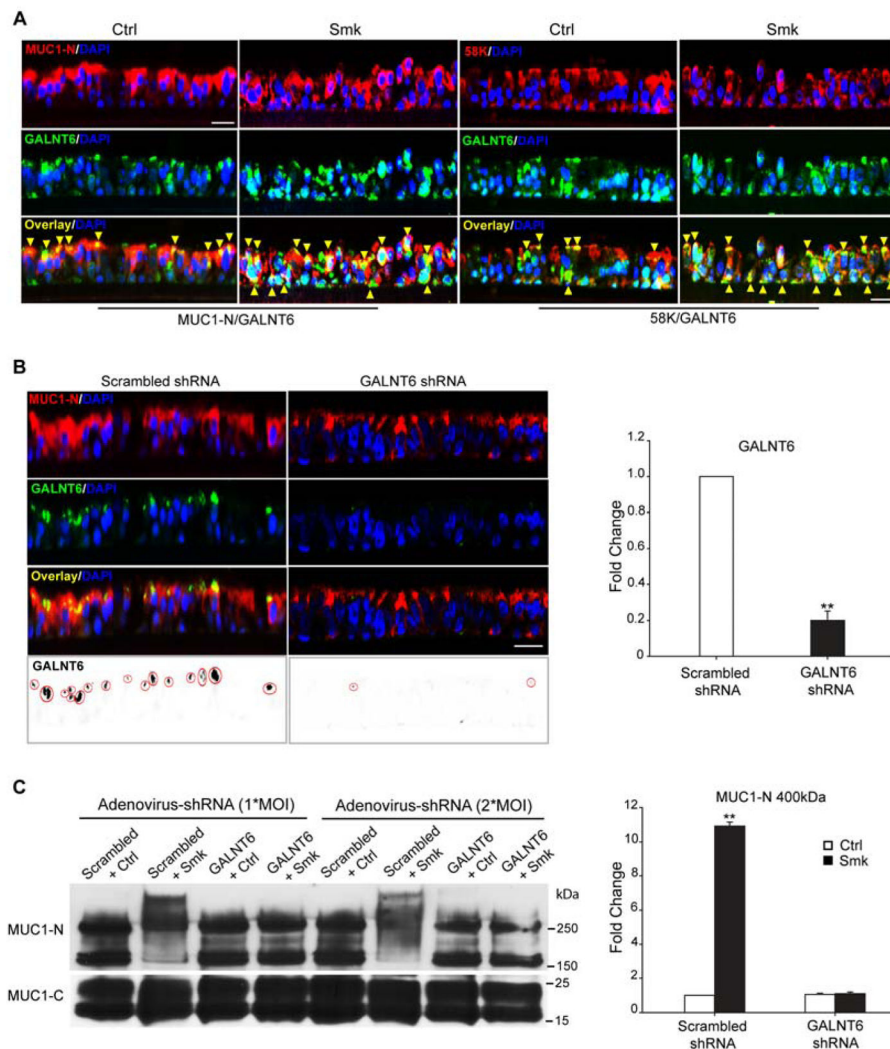
Figure 4.
Smoke provoked formation of MUC1-C/galectin-3/EGFR complexes in polarized HBE
cells. **(A)** HBE cells were treated with Ctrl or Smk medium at 23 (25%), 46 (50%) and 92
(100%) mg/m^3 total suspension particles (TSP) for 4h. MUC1-C IP was analyzed by WB
probed with galectin-3, EGFR and MUC1-C antibodies. Blots were stripped and reprobed
with TyrP antibodies (4G10, PY20 and PY100). Bands recognized by 4G10 overlapped with
EGFR (175kDa) and MUC1-C (20-25kDa) bands. Bands recognized by PY20 (20-25kDa)
and PY100 (20-25kDa) overlapped with each other and with MUC1-C. Equal loading was
confirmed with IgH bands. Quantitation of galectin-3, EGFR, EGFR-TyrP (4G10), MUC1-
C-TyrP (4G10) and MUC1-C-TyrP (PY100) pulled down by MUC1-C after 100% Smk
exposure was normalized to untreated control (designated as 1-fold) and reported as mean ±
SEM fold change. **p < 0.01, Smk-treated cells versus untreated Ctrl. **(B)** HBE cells were
treated with Ctrl or 100% Smk medium for 4h and immunostained with antibodies directed
against MUC1-C (red, top panels), galectin-3 (green, middle panels of left two lanes) or
EGFR (green, middle panels of right two lanes). Merged MUC1-C/galectin-3 signal (yellow,
bottom panels of left two lanes) indicates smoke-induced MUC1-C/galectin-3 interaction
(yellow arrowheads). Merged MUC1-C/EGFR signal (yellow, bottom panels of right two
lanes) demonstrates smoke-induced formation of MUC1-C/EGFR complexes (yellow
arrowheads). Cell nuclei were stained with DAPI (blue). Scale bar represents 50μm.

Figure 5.
Smoke-induced MUC1-C glycosylation modulates MUC1-C/galectin-3/EGFR complex
formation and Src/Jnk/MUC1-C signaling downstream of EGFR in polarized HBE cells.
(A–B) HBE cells were preincubated with TB or vehicle control (DMSO) overnight before
treating with Smk or Ctrl medium for 4h in the presence of TB. **(A)** MUC1-C IP was
analyzed with WB probed with galectin-3, EGFR, TyrP (4G10), Src and MUC1-C
antibodies. The 175kDa bands recognized by 4G10 completely overlapped with EGFR.
Equal loading was confirmed with IgH bands. Quantitation of MUC1-C bound galectin-3,
EGFR, EGFR-TyrP and Src after smoke and/or TB exposure was normalized to untreated
control (designated as 1-fold) and reported as mean ± SEM fold change. **(B)** WB probed
with TyrP (4G10), Tyr^{416}-phosphorylated Src (Src-P), Thr^{183}/Tyr^{185}-phosphorylated
SAPK/Jnk (Jnk-P) and MUC1-C antibodies. The 175kDa bands recognized by 4G10
completely overlapped with EGFR. Equal loading was confirmed with GAPDH.
Densitometric quantitation of EGFR-TyrP, Src-P and Jnk-P after smoke and/or TB treatment
was normalized to untreated control (designated as 1-fold) and graphed as mean ± SEM fold
change. **p < 0.01, Smk-treated cells versus untreated Ctrl.

Figure 6.
Adenovirus-delivered shRNA knockdown of GALNT6 in polarized HBE cells. **(A)** GALNT6 colocalized with MUC1-N and Golgi marker 58K. HBE cells were treated with Ctrl or Smk medium for 4h and immunostained with antibodies against MUC1-N (red, top panels of left two lanes), 58K (red, top panels of right two lanes), GALNT6 (green, middle panels). Merged MUC1-N/GALNT6 images (yellow signals, bottom panels of left two lanes) indicate MUC1-N colocalized with GALNT6 (yellow arrowheads) before and after smoke treatment. Merged 58K/GALNT6 images (yellow signals, bottom panels of right two lanes) demonstrate localization of GALNT6 in Golgi before and after smoke exposure (yellow arrowheads). Cell nuclei were stained with DAPI (blue). Scale bar represents 50μm. **(B)** Pseudostratified HBE cells were infected with 1*MOI (multiplicity of infectivity) adenovirus-delivered scrambled shRNA or GALNT6 shRNA overnight, followed by 4 days in culture. Immunostaining of MUC1-N (red, top row), GALNT6 (green, 2nd row), and merged MUC1-N/GALNT6 (yellow, 3rd row) indicate colocalization. Nuclei were visualized with DAPI (blue). Scar bar represents 50μm. Monochrome images of GALNT6 were inverted to black signals (red circles, bottom panels) and quantitated with ImageJ

software. Knocking down GALNT6 in GALNT6 shRNA-treated cells was compared to scrambled shRNA-treated control (designated as 1-fold) and graphed as mean ± SEM fold change. **p < 0.01, GALNT6 shRNA-treated cells versus scrambled shRNA control. **(C)** Polarized HBE cells were infected with 1*MOI or 2*MOI of adenovirus-delivered scrambled shRNA or GALNT6 shRNA overnight and cultured for another 4 days. Cells treated with Smk or Ctrl medium for 4h were IP'd with MUC1-C and probed with MUC1-N and MUC1-C antibodies. Densitometric quantitation of the 400kDa MUC1-N band (mean ± SEM, **p < 0.01) compared to scrambled shRNA/Ctrl exposed cells (designated as 1-fold),
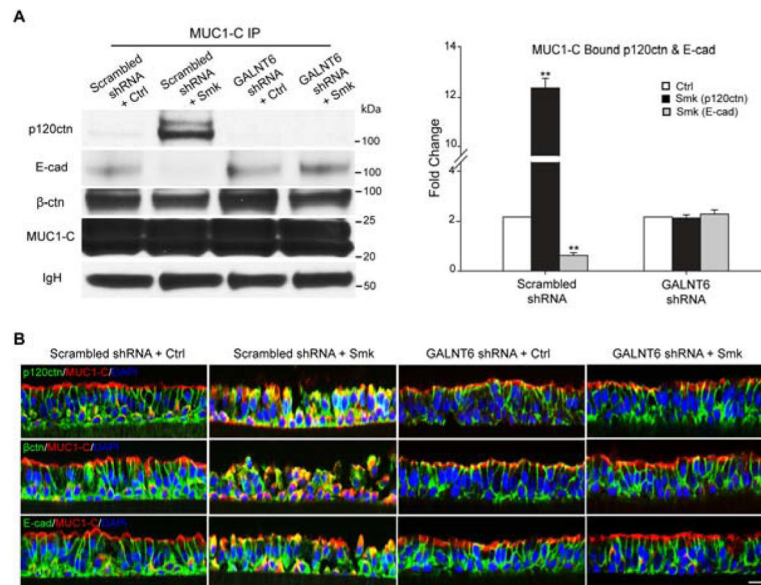
Figure 7.
Suppression of smoke-induced MUC1-N glycosylation abolished smoke-provoked MUC1-C/p120ctn interaction and E-cad loss in polarized HBE cells. **(A–B)** Polarized HBE cells were infected with 1*MOI of adenoviral scrambled shRNA or GALNT shRNA overnight and cultured for another 4 days before exposing to Ctrl or Smk medium for 4h. **(A)** The cell lysates were IP'd with anti-MUC1-C followed by WB probed with p120ctn, E-cad, β-ctn and MUC1-C antibodies. Equal loading was confirmed with IgH bands. Densitometric quantitation (mean ± SEM fold change, **p < 0.01) of MUC1-bound p120ctn (black columns) and E-cad (gray columns). **(B)** Immunofluorescent staining of polarized HBE cells exposed to scrambled shRNA/Ctrl, scrambled shRNA/Smk, GALNT6 shRNA/Ctrl and GALNT6 shRNA/Smk for p120ctn (green, top panels), β-ctn (green, middle panels), E-cad (lower panels) and MUC1-C (red, all panels), DAPI nuclear counterstain (blue). Scale bar represents 50μm.
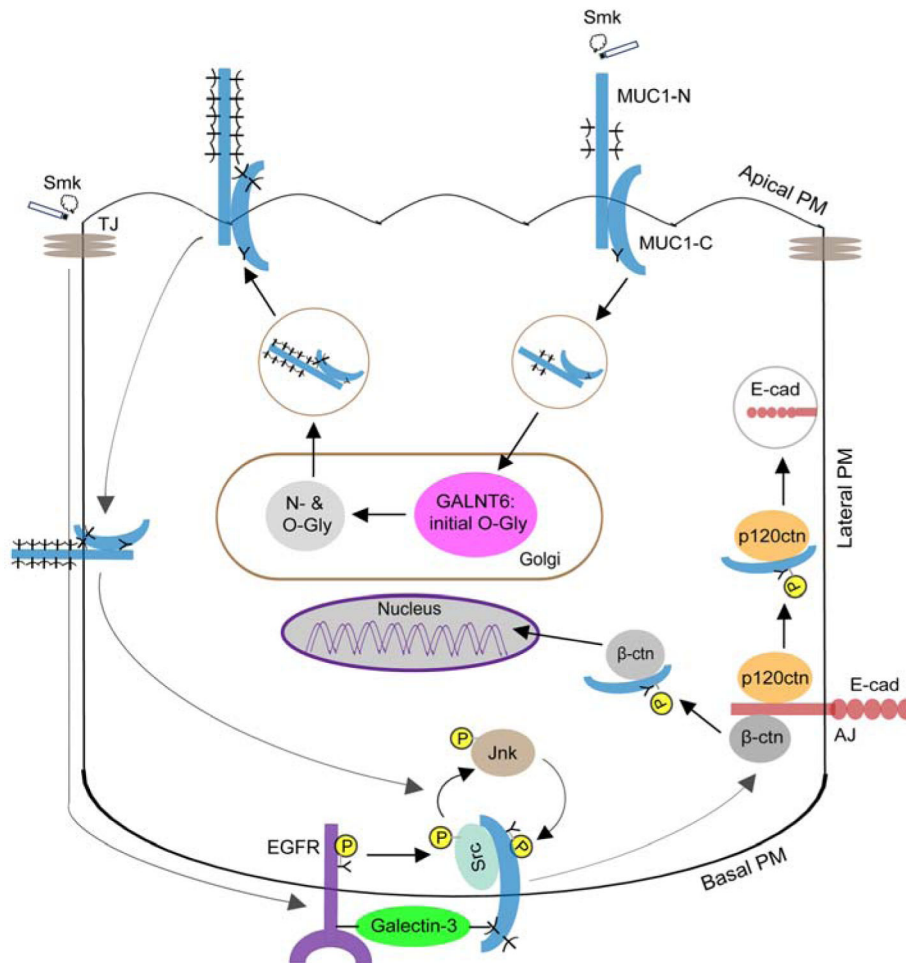
Figure 8.
Schematic representation of smoke-provoked MUC1 glycosylation in regulation of MUC1-C/p120ctn interaction and adherens junction (AJ) disruption. MUC1 is localized on the apical plasma membrane (PM) of polarized HBE cells as a MUC1-N/MUC1-C heterodimer where it is spatially segregated from AJs and EGFR on the basolateral PM. Cigarette smoke (Smk) stimulates internalization of MUC1 and its intracellular trafficking to the Golgi, where MUC1 is initially O-glycosylated (O-Gly) by GALNT6 and further N- (N-Gly) and O-glycosylated by other enzymes. In response to smoke, fully glycosylated MUC1 is sent back to apical PM and subsequently translocated to basolateral PM, where MUC1-C, EGFR and galectin-3 form a signalosome through the bridging of their sugar moieties following smoke-induced shedding of MUC1-N. Src is also recruited to the MUC1-C/EGFR/galectin-3 complex by smoke where it binds the cytoplasmic tail of MUC1-C (MUC1-CT). Smoke destroys tight junctions (TJs) and gains access to basolateral EGFR through increased paracellular permeability. MUC1-C is then activated through tyrosine phosphorylation (Y-P) by smoke-induced EGFR/Src/Jnk signaling. Activation of MUC1-C promotes its interaction with p120ctn and β-ctn at AJs. MUC1-C/p120ctn interaction exposes ubiquitin ligation sites of E-cad and thereby results in proteasomal degradation of E-cad, a hallmark of EMT [12]. MUC1-C/β-ctn interaction facilitates β-ctn's entry into nucleus and activates the Wnt

signaling pathway leading to cell proliferation and migration [11]. Blocking smoke-induced MUC1 glycosylation through GALNT6 knock down prevents the loss of Ecad and restores AJ integrity. Thus, targeting the initiating O-glycosylation step of MUC1 may provide a novel therapeutic approach to prevent smoke-induced EMT and early lung carcinogenesis.